Surface Adhesion

Deutsche Ausgabe: DOI: 10.1002/ange.201603906
Internationale Ausgabe: DOI: 10.1002/anie.201603906

Dynamic Self-Assembly Adhesion of a Paraquat Droplet on a Pillar[5]arene Surface

*Li Luo, Guanrong Nie, Demei Tian, Hongtao Deng, Lei Jiang, and Haibing Li**

Abstract: *The adhesion of herbicide droplets on leaf surfaces plays an important role in the herbicide's adsorption by crops. How to control the adhesive binding which occurs through dynamic self-assembly between the macroscopic droplet and the surface is a challenging task. We introduce a host onto surfaces that controls the binding of guests in the paraquat droplets. The pillar[5]arene-functional surface showed the selective binding of paraquat droplets via the host–guest interaction. The work is promising for improving the efficiency of herbicides.*

The self-assembly of macroscopic droplets is of long-standing and continuing interest owing to its fundamental and technological relevance.[1–3] For example, the attachment of herbicide droplets on leaf surfaces by self-assembly plays an important role in the adsorption of the herbicide by crops, as it can reduce the amount of herbicide[4–6] required. So far, the study of the self-assembly processes mainly focused on static structures,[7–10] but dynamic systems are largely unexplored and pose a great challenge. For instance, how to control the dynamic self-assembly of specific herbicide droplet on the surface?

Paraquat is a widely used herbicide.[11–14] To address the challenging problem, we introduce host–guest chemistry onto surfaces to control the dynamic self-assembly binding of the paraquat droplet to the surface. The pillar[*n*]arenes,[15–19] composed of hydroquinone unit linked by methylene bridges at *para* positions, are rigid as well as easily functionalized with various substituents.[20,21] The unique cavity structure and easy modification of pillar[*n*]arenes endow them with an outstanding ability to selectively bind different kinds of guests,[22–24] which provides a useful platform for the construction of the functional surface.

Herein, an inclinable pillar[5]arene-modified silicon surface was fabricated to accomplish the selective dynamic self-assembly adhesion of paraquat droplets to the surface via the host–guest interaction. The pillar[5]arene (**P5A**) was synthesized by the synthetic route shown in Figure S1 of the Supporting Information. The ^{1}H NMR, ^{13}C NMR, and mass spectra (Figure S2,S3,S4) confirmed the structure of **P5A**. The alkynyl group at lower rim of **P5A** was used to link with the silicon surface and the electron-rich cavity of **P5A** served as the recognition unit. Then, the **P5A** was bonded onto the silicon surface by the click reaction.[25] The **P5A**-functional surface can induce the dynamic self-assembly binding of specific paraquat droplet (Scheme 1).

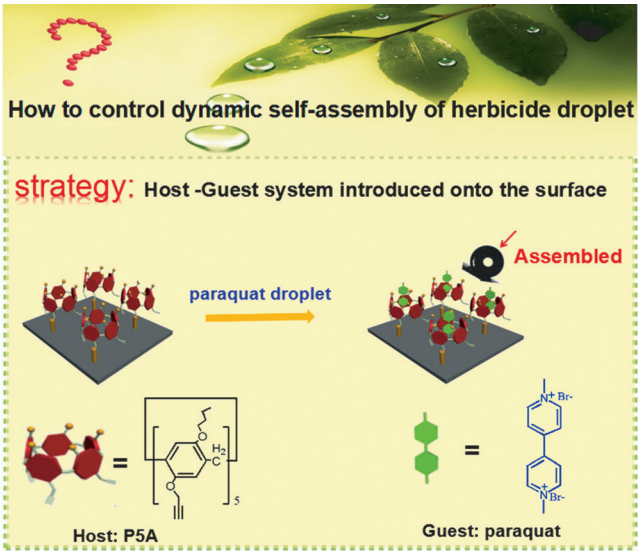

Scheme 1. Schematic illustration of the dynamic self-assembly of paraquat-droplet–surface complex.

The interaction between **P5A** and methyl paraquat (**G2**) was investigated in solution phase by UV and ^{1}H NMR spectroscopy and mass spectrometry (MS). The UV analysis of the **P5A** and different paraquat derivatives was carried out. As shown in Figure 1 b, after adding the **G2** into **P5A** solution, the UV spectra presented a new peak at 243 nm. However, there were no changes at 243 nm for other guests. Furthermore, the association constant of **P5A** and **G2** determined by UV continuous titration is $(1.32\pm0.08)\times10^3\,\text{M}^{-1}$, which is bigger than that of **P5A** and **G1**, **G3**, **G4**, **G5** ($(3.73\pm0.03)\times10^2$, $(1.35\pm0.05)\times10^2$, $(2.67\pm0.02)\times10^2$, $(2.46\pm0.03)\times10^2\,\text{M}^{-1}$ respectively)as shown in Figure S5. Further, the complex ratio of **P5A** and **G2** was determined to be 1:1 by Job's plot (Figure S6). ^{1}H NMR experiments are shown in Figure 2. The **G2a**, **G2b** and **G2c** protons of **G2** underwent upfield shifts of 0.08 ppm and 0.05 ppm, respectively, meanwhile the H_1 protons underwent upfield shift of 0.12 ppm and the H_2, H_3 protons of **P5A** shifted downfield by 0.03 ppm,

[*] L. Luo, G. R. Nie, Dr. D. M. Tian, Dr. H. T. Deng, Prof. H. B. Li
Key Laboratory of Pesticide and Chemical Biology (CCNU), Ministry of Education, College of Chemistry, Central China Normal University
Wuhan 430079 (P.R. China)
E-mail: lhbing@mail.ccnu.edu.cn
Prof. L. Jiang, Prof. H. B. Li
Beijing National Laboratory for Molecular Sciences (BNLMS), Key Laboratory of Organic Solids, Institute of Chemistry, Chinese Academy of Sciences
Beijing, 100190 (P.R. China)

Supporting information for this article can be found under: http://dx.doi.org/10.1002/anie.201603906.

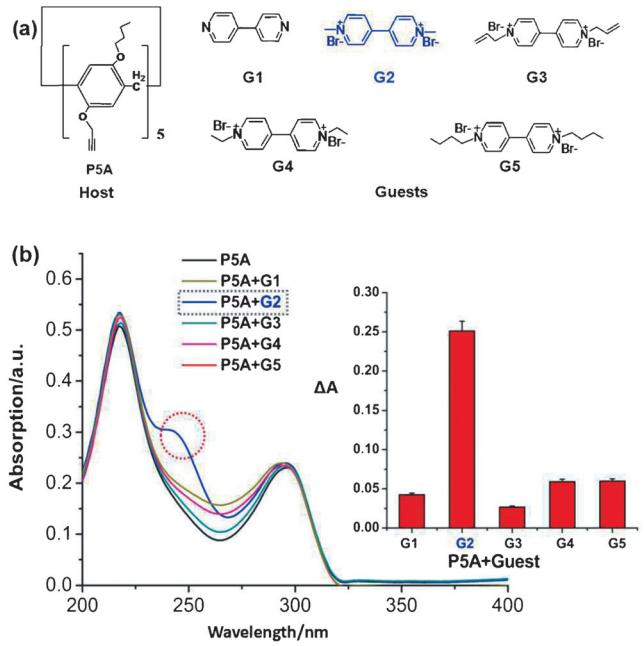

Figure 1. a) The chemical structures of the tested host and guests; b) the UV spectra of **P5A** after adding different guests. The difference value ΔA $((A_{243}/A_{217})_{P5A+Guest}-(A_{243}/A_{217})_{P5A})$ was shown in the column diagram after the different guest was added into P5A solution showing **P5A** is selective to **G2**. The dotted circle highlights the new signal at 243 nm.

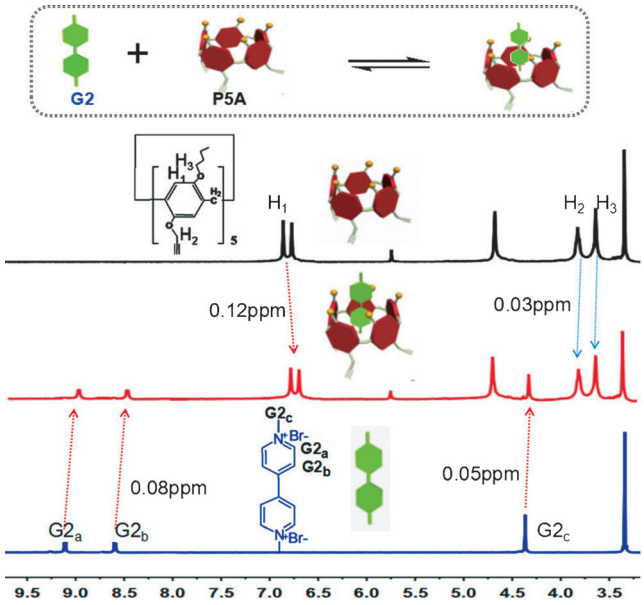

Figure 2. The ^{1}H NMR spectra of **P5A** (black spectrum; 30 mM, $CD_3CN:D_2O=50:1$, 400 MHz, 298 K), **G2** (blue spectrum; 30 mM, $CD_3CN:D_2O=50:1$, 400 MHz, 298 K). And a mixture of **P5A** and **G2** (red).

which are in accord with the literature.[26] It was deduced that **G2** entered into the cavity of **P5A**. The MS (Figure S7) and ^{1}H NMR titration test (Figure S8) of **P5A** and **G2** were conducted to further confirm the interaction and 1:1 complex stoichiometry. Furthermore, the binding of **P5A** with **G2** was also examined by Gaussian03 calculations (Figure S9). All the energy were obtained by the equation of $\Delta E_{(\text{binding energy})} = E_{(\text{host-guest})}-(E_{\text{host}}+E_{\text{guest}})$. The binding energy of P5A and **G2** ($-210.04\ \text{kJ mol}^{-1}$) is smaller than the binding energy of **P5A** and other guests, indicating the complex of **P5A** with **G2** is more stable. These results indicate the host **P5A** selectively binds to **G2**.

The micro-structured silicon surfaces, which mimic the surfaces of leaves,[4–6] have been selected as a substrate. The silicon surface topography was observed by SEM (Figure S10). The **P5A**-functionalized silicon surface was constructed by click reaction. After the bare silicon surface was deposited, as can be seen in Figure S11, the hydrophilic hydroxy groups are exposed on surface where the measured contact angle (CA) was $8.2\pm3.0°$. Then, the surface was modified with azide and the azide groups ($-N_3$) were exposed on the surface, giving rise to the increase of hydrophobicity so that the contact angle increased to $77.3\pm3.0°$. Finally, the host **P5A** was added to the surface by the click reaction between the $-N_3$ and the alkynyl group ($-C\equiv CH$) of **P5A**. The introduction of the hydrophobic **P5A** onto the surface caused the contact angle to further increase to $142.7\pm3.0°$, which suggested a super-hydrophobic surface was successfully fabricated. To further confirm the **P5A** was successfully attached to the surface, additional evidence was provided by XPS (Figure S12) and FTIR (Figure S13). As show in Figure S12, the XPS results showed that the content of carbon, oxygen, and nitrogen on surface changed before and after modification, which indicated the **P5A** was successfully added to the surface. As can be seen in Figure S13, the $-N_3$ peak at $2100\ \text{cm}^{-1}$ observed suggests that the $Si-N_3$ was formed successfully. After the **P5A** was added, the $-N_3$ peak at $2100\ \text{cm}^{-1}$ distinctly weakened, while the peak of the benzene skeleton vibration near $1500\ \text{cm}^{-1}$ was observed, which indicated the **P5A** was modified on the surface.

Subsequently, we investigated the self-assembly of the paraquat-derivative droplets with the concentration of 10^{-3} M on the flat **P5A**-modified surface. As shown in Figure S14, there are no distinctive difference by the measurement of static contact angles after the guests and pure water droplet was added to the **P5A** surface. However, the contact angle hysteresis (CAH) in Figure S15 is much different. The measured CAH were 8.4°, 9.9°, 10.4°, 9.4°, 11.1°, respectively after adding pure water, **G1**, **G3**, **G4**, and **G5** droplets to the **P5A**-modified surface, while the CAH was 45.3° after adding **G2** droplets, which is much higher than that of the pure water droplet and the other guests. According to the formula:[27] $\sin\alpha=\omega\gamma\text{LA}\,(\cos\theta_{\text{rec}}-\cos\theta_{\text{adv}})/mg$, where α means the sliding angle, ω is the width of the droplet, γLA is surface tension of the droplet, θ_{rec} (θ_{adv}) is the receding (advancing) contact angle, m is the mass of the droplet and g is the gravity acceleration, the theoretical sliding angle of the different droplets on the **P5A** surface was calculated. As shown in Figure S16, the sliding angle of pure water droplet, **G1**, **G3**, **G4** and **G5** droplet was about 7°, 13°, 10°, 12° and 10°, respectively, on the **P5A** surface, while the sliding angle of **G2** droplet was about 56°. Therefore, we tilted the **P5A**-modified to 45° to observe the dynamic assembly behavior of guest droplet. As shown in Figure 3a, the pure water, **G1**, **G3**, **G4**,

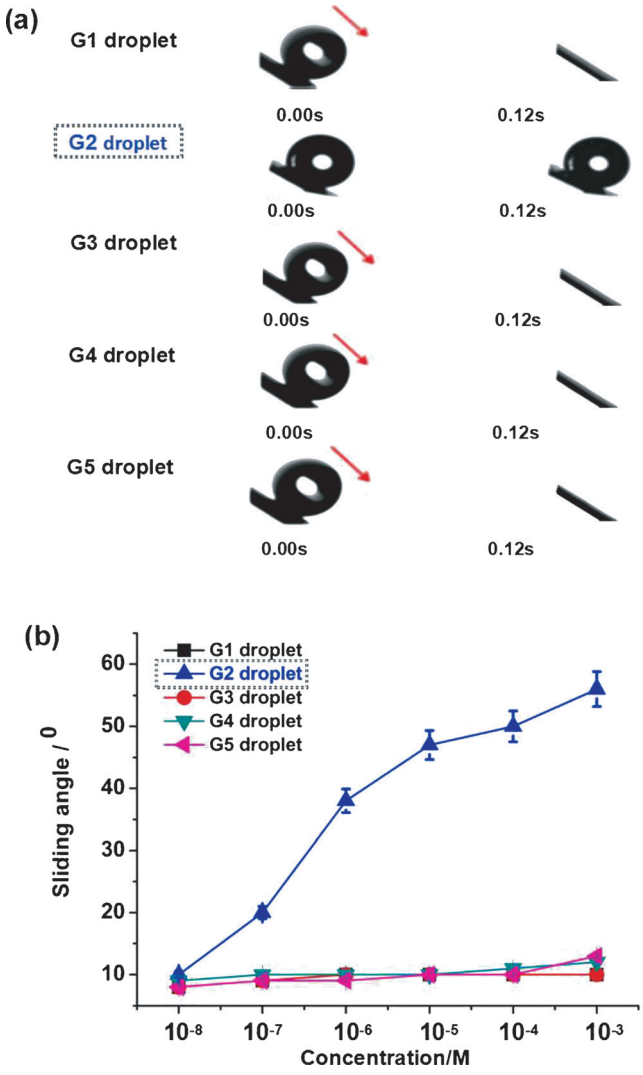

Figure 3. The selectivity of the **P5A**-functional surface to **G2** droplets: a) the **G1**, **G2**, **G3**, **G4**, **G5** behavior on the **P5A**-modified surface tilted to 45°; b) The sliding-angle change of the different guest droplets with varying concentrations (1.0×10^{-8}–1.0×10^{-3} M) on the **P5A**-modified surface showing the selective adhesion of the **G2** droplet.

G5 droplets slide quickly off the surface. However, the **G2** droplet stayed on the surface by the assemble adhesion. The sliding and assemble adhesion process of the droplets with time are shown in Figure S17. Moreover, it is found that the sliding angle of the droplet changes with the increasing concentration of the guest in the droplets. As can be seen in Figure 3b, the sliding angles of the **G1**, **G3**, **G4**, **G5** droplets did not change significantly whereas the sliding angle of the **G2** droplet increased with the increasing guest concentration of the droplets(10^{-8} M–10^{-3} M).

The possible mechanism is shown in Figure 4. The paraquat molecules in droplet bind with the functional surface by the host–guest interaction to form the stable complex with the system energy reducing. Because the binding strength of **G2** with **P5A** is stronger than the other guests, the **G2** molecules in droplet is easier to assemble with the **P5A** modified on the surface to generate the enough binding force to resist the droplet gravity. Hence, the **G2** droplet can stay on the inclined

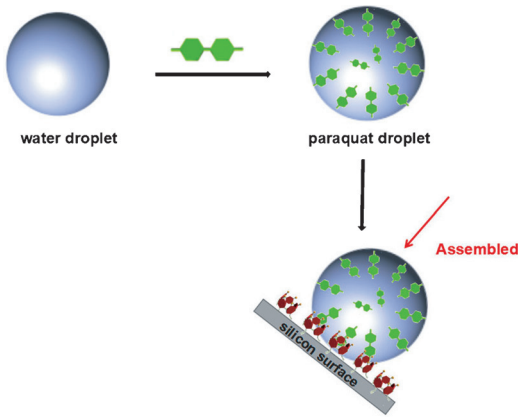

Figure 4. Schematic representation of the possible mechanism for the binding of the **G2** droplet to the **P5A**-modified surface.

surface. However, the other droplets can slide off the surface because their binding strength on **P5A** surface is too low to resist the droplet gravity.

Meanwhile, the sliding angle of the **G2** droplet increased with the increasing concentration of guest in the droplets, which is a result of more **G2** molecules being able to bind with the **P5A**-functional surface thereby increasing the binding strength to prevent the droplet from sliding.

To verify the binding strength of the pesticide guests on the **P5A** surface, the quartz crystal microbalance (QCM) was used to study the behavior of paraquat pesticides on pillar[5]arene-modified surfaces. In this experiment, pillar[5]arene coated quartz crystals were obtained by the reaction between the terminal alkyne groups of pillar[5]arene and the gold layer on crystals.[28] As shown in Figure S18, the **G2** exhibited distinctly stronger adsorption on pillar[5]arene surface with the biggest binding constant 145.4 M^{-1} than other paraquat derivates.

The surface can be reused to adhere to **G2** droplets after washing the surface by water. Therefore, the repeatability of this phenomenon was investigated as shown in Figure S19. Upon alternately adding pure water and **G2** droplets, the **P5A**-functional surface, tilt angle of 45°, can still adhere to **G2** droplets after seven cycles, which suggests that the **P5A** constructed surface is stable.

In conclusion, **P5A** was synthesized and the **P5A**-functional surface was constructed by the click reaction to investigate the dynamic self-assembly adhesion of paraquat droplets. The **P5A**-functional surface exhibited the dynamic self-assembly adhesion of specific methyl paraquat droplets **G2** because of the matched host–guest interaction between **P5A** and **G2**. The fabricated surface is promising in the application of the rapid detection of paraquat for environmental monitoring and provides an approach for improving the utilization efficiency of herbicide.

Acknowledgements

This work was financially supported by the National Natural Science Foundation of China (21572076, 21372092), Natural

Science Foundation of Hubei Province (2013CFA112, 2014CFB246), Wuhan scientific and technological projects (2015020101010079) and Self-determined research funds of CCNU from the colleges' basic research and operation of MOE (CCNU15KFY005).

Keywords: dynamic self-assembly · host–guest systems · paraquat · pillar[5]arenes · surface adhesion

How to cite: *Angew. Chem. Int. Ed.* **2016**, *55*, 12713–12716
Angew. Chem. **2016**, *128*, 12905–12908

[1] N. Bowden, I. S. Choi, B. A. Grzybowski, G. M. Whitesides, *J. Am. Chem. Soc.* **1999**, *121*, 5373–5391.
[2] T. Shinbrot, *Nature* **1997**, *389*, 574–576.
[3] M. M. Burns, J. M. Fournier, J. A. Golovchenko, *Science* **1990**, *249*, 749–754.
[4] G. Qing, X. Wang, L. Jiang, H. Fuchs, T. Sun, *Soft Matter* **2009**, *5*, 2759–2765.
[5] G. Qing, T. Sun, *Angew. Chem. Int. Ed.* **2014**, *53*, 930–932; *Angew. Chem.* **2014**, *126*, 946–948.
[6] a) N. M. Feng, H. Y. Zhao, J. Y. Zhan, D. M. Tian, H. B. Li, *Org. Lett.* **2012**, *14*, 1958–1961; b) X. Y. Zhang, J. Li, N. M. Feng, L. Luo, Z. Dai, L. Yang, D. M. Tian, H. B. Li, *Org. Biomol. Chem.* **2014**, *12*, 6824–6830; c) X. F. Zeng, J. K. Ma, L. Luo, L. L. Yang, X. L. Cao, D. M. Tian, H. B. Li, *Org. Lett.* **2015**, *17*, 2976–2979.
[7] S. Jakubith, H. H. Rotermund, W. Engel, A. von Oertzen, G. Ertl, *Phys. Rev. Lett.* **1990**, *65*, 3013–3016.
[8] B. A. Grzybowshi, H. A. Stone, G. M. Whitesides, *Nature* **2000**, *405*, 1033–1036.
[9] C. Howell, T. L. Vu, C. P. Johnson, X. Hou, O. Ahanotu, J. Alvarenga, *Chem. Mater.* **2015**, *27*, 1792–1800.
[10] X. Hou, Y. Hu, A. L. Grinthal, *Nature* **2015**, *519*, 70–73.
[11] W. Rongchapo, O. Sophiphun, K. Rintramee, S. Prayoonpokarach, *Water Sci. Technol.* **2013**, *68*, 863–869.
[12] T. R. Hawkes, *Pest Manage. Sci.* **2014**, *70*, 1316–1323.
[13] Y. Huang, C. Li, Z. Lin, *ACS Appl. Mater. Interfaces* **2014**, *6*, 19766–19773.
[14] Q. Li, X. J. Peng, H. Yang, H. B. Wang, Y. Shu, *Mol. Pharm.* **2011**, *8*, 2476–2483.
[15] N. L. Strutt, H. C. Zhang, S. T. Schneebeli, J. F. Stoddart, *Acc. Chem. Res.* **2014**, *47*, 2631–2642.
[16] T. Ogoshi, S. Kanai, S. Fujinami, T. Yamagishi, Y. Nakamoto, *J. Am. Chem. Soc.* **2008**, *130*, 5022–5023.
[17] D. Cao, Y. Kou, J. Liang, Z. Chen, L. Wang, H. Meier, *Angew. Chem. Int. Ed.* **2009**, *48*, 9721–9723; *Angew. Chem.* **2009**, *121*, 9901–9903.
[18] X. B. Hu, L. Chen, W. Si, Y. Yu, J. L. Hou, *Chem. Commun.* **2011**, *47*, 4694–4696.
[19] N. L. Strutt, R. S. Forgan, J. M. Spruell, Y. Y. Botros, J. F. Stoddart, *J. Am. Chem. Soc.* **2011**, *133*, 5668–5671.
[20] M. Barboiu, *Angew. Chem. Int. Ed.* **2012**, *51*, 11674–11766; *Angew. Chem.* **2012**, *124*, 11842–11844.
[21] T. Ogoshi, S. Takashima, T. Yamagishi, *J. Am. Chem. Soc.* **2015**, *137*, 10962–10964.
[22] T. Ogoshi, R. Sueto, K. Yoshikoshi, Y. Sakata, S. Akine, T. Yamagishi, *Angew. Chem. Int. Ed.* **2015**, *54*, 9849–9852; *Angew. Chem.* **2015**, *127*, 9987–9990.
[23] G. C. Yu, X. Y. Zhou, Z. B. Zhang, C. Y. Han, Z. W. Mao, C. Y. Gao, F. H. Huang, *J. Am. Chem. Soc.* **2012**, *134*, 19489–19497.
[24] Z. Zhang, Y. Luo, J. Chen, S. Dong, Y. Yu, Z. Ma, F. Huang, *Angew. Chem. Int. Ed.* **2011**, *50*, 1397–1401; *Angew. Chem.* **2011**, *123*, 1433–1437.
[25] B. Yameen, M. Ali, A. Marta, R. Neumann, W. Ensinger, W. Knoll, O. Azzaroni, *Polym. Chem.* **2010**, *1*, 183–192.
[26] X. D. Chi, M. Xue, Y. Yao, F. H. Huang, *Org. Lett.* **2013**, *15*, 4722–4725.
[27] C. G. L. Furmidge, *J. Colloid Sci.* **1962**, *17*, 309–324.
[28] S. Zhang, K. L. Chandra, C. B. Gorman, *J. Am. Chem. Soc.* **2007**, *129*, 4876–4877.

Received: April 22, 2016
Published online: June 29, 2016

